TIN SULPHIDE NANOSTRUCTURES SYNTHESIZED BY CHEMICAL BATH DEPOSITION FOR NEAR-INFRA-RED PHOTODETECTOR APPLICATIONS

by

MOHAMED SALEH MAHDI

Thesis submitted in fulfilment of the requirements
for the degree of
Doctor of Philosophy

DECEMBER 2017

ACKNOWLEDGEMENT

First, I wish to thank Allah for the good health, patience, and well being that were necessary to complete this research. Second, I would like to express my sincere thanks to my main supervisor Dr. Naser Mahmoud Ahmed for his kind cooperation, useful contribution, and valuable guidance during my study and research work. I also wish to record my deep sense of gratitude to my co-supervisors prof. Dr. Kamarulazizi Ibrahim and Dr. Arshad Hmood for their useful and valuable suggestions, inspiring guidance, and consistent encouragement. They always taught me how to face hard moments in this research. Third, I am profoundly thankful to my immediate family to whom this dissertation is dedicated; they have been a constant source of love, concern, support, and strength during all these years. I would like to express my heartfelt gratitude to my family. Finally, I would like to express my gratitude to the technical staff, who maintained all the machines in the N.O.R lab very efficiently. I feel that they are the greatest system administrators in Malaysia: from Abdul Jamil to Yushamdan, Ee Bee Choo, and the rest of the team.

Mohamed Saleh Mahdi
December 2017
Penang-Malaysia

TABLE OF CONTENT

LIST OF TABLES

LIST OF FIGURES

LIST OF SYMBOLS

Å	Angstrom
a.u.	Arbitrary unit
E_g	Band gap energy
V	Bias voltage
θ	Bragg's angle
^oC	Celsius temperature
E_C	Conduction band
σ	Conductivity
D	Crystallite size
I_{dark}	Dark current
R_∞	Diffuse reflectance
χ	Electron affinity
A_l	Effective illuminated area
μ_n	Electron mobility
eV	Electron volt
ν	Frequency
β	Full width at half maximum
μ_p	Hole mobility
P_λ	Illumination intensity
I_o	Intensity of the incident light
I	Intensity of the transmission light
d_{hkl}	Inter-plane distance
a, b, c	Lattice constants

ε	Strain
I_{light}	Light current
h, k, l	Miller indices
μ	Mobility
M	Molar
φ_m	Metal work function
Φ	Photon flux density
h	Planck's constant
R	Responsivity
d	Separation between the electrodes
χ	Semiconductor electron affinity
φ_s	Semiconductor work function
S	Sensitivity
T_C	Texture coefficient
t	Thickness
T_t	Transit time
T	Transmittance
E_V	Valence band
W/cm^2	Watt/ Centimeter square
λ	Wavelength

LIST OF ABBREVIATIONS

CBD	Chemical bath deposition
DC	Direct current
EDX	Energy dispersive X-ray
EDTA	Ethylene diamine tetra-acetic acid
FESEM	Field emission scanning electron microscopy
F(R)	Kubelka-Munk function
LED	Light emitting diode
MSM	Metal semiconductor metal
NIR	Near infrared
PET	Polyethylene terephthalate
RF	Radio frequency
TEA	Triethanolamine
TSC	Trisodium citrate
UV	Ultraviolet
Vis	Visible
XRD	X-ray diffraction

NANOSTRUKTUR STANUM SULFIDA DISINTESISKAN MELALUI PEMENDAPAN RENDAMAN KIMIA UNTUK APLIKASI FOTOPENGESAN INFRAMERAH HAMPIR

ABSTRAK

Kajian ini bertujuan untuk mengoptimumkan parameter pertumbuhan untuk mensintesis filem nipis nanostruktur Stanum Sulfida (SnS) untuk alat fotopengesan yang berkesan. Kualiti kristal yang baik dan arus gelap yang rendah merupakan syarat-syarat penting untuk memperoleh prestasi tinggi peranti fotopengesan. Selain itu, pertumbuhan filem nipis pada suhu rendah membolehkan penggunaan bahan Polietilena Tereftalat (PET) sebagai substrat. Pertumbuhan filem nipis dicapai dengan menggunakan teknik Pemendapan Rendaman Kimia (CBD). Pertama sekali, peningkatan kehabluran filem nipis nanostruktur SnS pada substrat kaca dengan menggunakan teknik CBD, serta mengubah kepekatan (0.15-0.21 M) sitrat trinatrium (TSC) tidak toksik sebagai agen kompleks telah ditunjukkan. Dalam pada itu, corak-corak pembelauan sinar-x (XRD) menunjukkan struktur ortorombus filem nipis nanostruktur SnS yang disintesiskan. Selain itu, fasa-fasa stanum sulfida (SnS dan Sn_2S_3) dapat dikawal dengan mudah dengan mengubah kepekatan agen kompleks, di mana keamatan puncak Sn_2S_3 semakin menurun secara beransur-ansur sehingga hampir hilang apabila kepekatan TSC meningkat daripada 0.15 M hingga 0.21 M. Selain itu, jurang jalur tenaga filem nipis dialihkan kepada tenaga yang lebih rendah apabila kepekatan TSC meningkat daripada 0.15 M hingga 0.21 M. Dalam pada itu, fotopengesan yang dihasilkan pada kepekatan optimum TSC menunjukkan sifat fotorespon yang baik di bawah pencahayaan inframerah hampir (850 nm). Kedua, peralihan daripada struktur ortorombus kepada struktur kubik telah berjaya dijalankan

dengan mengubah nilai pH (5-7.5) larutan tindak balas atas kaca dan substrat PET. Peralihan ini berlaku pada pH 7 dan menyebabkan pengurangan yang bermakna bagi magnitud arus gelap dalam fotopengesan yang dihasilkan, daripada µA kepada nA untuk kaca, serta daripada nA kepada pA untuk substrat PET masing-masingnya. Hasilnya, fotopengesan yang berasaskan struktur kubik menunjukkan kefotopekaan yang lebih tinggi dan masa respon yang lebih cepat berbanding fotopengesan yang berasaskan struktur ortorombus. Imej FESEM filem menunjukkan morfologi nano-emping; namun begitu, penukleusan dan pertumbuhan filem berubah daripada mekanisma kluster demi kluster kepada mekanisma ion demi ion pada nilai pH 7. Dalam pada itu, untuk kedua-dua substrat, jurang jalur tenaga filem nipis telah dialihkan ke tenaga lebih tinggi apabila pH dinaikkan daripada 5 kepada 7.5. Nilai kepekaan fotopengesan yang dihasilkan pada substrat PET dicatatkan pada lebih kurang 2990%, 1604%, 2591% dan 446% pada pencahayaan diod pemancar cahaya 380, 530, 750 dan 850 nm masing-masingnya pada voltan pincang 3V. Keputusan yang diperoleh mencadangkan bahawa nanostruktur SNS struktur kristal kubik mempunyai masa depan yang cerah dalam bidang peranti fotopengesan dan optoelektronik respon jalur lebar.

TIN SULPHIDE NANOSTRUCTURES SYNTHESIZED BY CHEMICAL BATH DEPOSITION FOR NEAR-INFRA-RED PHOTODETECTOR APPLICATIONS

ABSTRACT

This study aims to optimize the growth parameters for synthesizing nanostructured tin sulphide (SnS) thin films for efficient photodetector devices. A good crystal quality and low dark current are significant prerequisites in obtaining a high photodetector device performance. In addition, low temperature growth of thin film allows the use of polyethylene terephthalate (PET) material as a substrate. The growth of thin films was achieved using chemical bath deposition technique (CBD). Firstly, the improvement of crystallinity of SnS nanostructure thin films on glass substrates using CBD technique, and changing the concentration (0.15-0.21 M) of non-toxic trisodium citrate (TSC) as complex agent has been demonstrated. Moreover, the x-ray diffraction (XRD) patterns revealed the orthorhombic structure of the synthesized SnS nanostructure thin films. Furthermore, tin sulphide phases (SnS and Sn_2S_3) can be easily controlled by changing the concentration of the complex agent, in which the Sn_2S_3 peak intensity, gradually declined in intensity until almost disappearing as the TSC concentration increased from 0.15 M to 0.21 M. Moreover, the energy band gap of thin films is shifted to lower energy as the TSC concentrations increased from 0.15 M to 0.21 M. In addition, the fabricated photodetector at optimum concentration of TSC revealed a good photoresponse properties under illumination of near infrared (850 nm). Secondly, the transition from an orthorhombic structure to a cubic structure was successfully performed by changing the pH value (5-7.5) of reaction solution on glass and PET substrates. This transition was at pH 7 and resulted

into a significant reduction in the magnitude of dark current of fabricated photodetectors from μA to nA, for glass and nA to pA, for PET substrates, respectively. As a result, the photodetectors based on cubic structure exhibited higher photosensitivity and faster response time compared to the photodetector based on orthorhombic structure. The FESEM images of the films showed the nanoflakes morphology; however, the nucleation and growth of films changed from cluster by cluster to ion by ion mechanism at the pH value 7. Moreover, for both substrates, the energy band gaps of thin films are shifted to higher energies as pH increased from 5 to 7.5. The sensitivity values of the fabricated photodetector on PET substrate were obtained to be approximately 2990%, 1604%, 2591% and 446% under illumination of light emitting diodes 380, 530, 750 and 850 nm at a bias voltage of 3 V respectively. The obtained results suggest that cubic crystal structure SnS nanostructure has a bright future in the field of broadband response photodetectors and optoelectronics devices.

CHAPTER 1: INTRODUCTION

1.1 Introduction

Environmentally benign materials such as tin sulphide (SnS) have garnered much interest in the manufacture of optoelectronic devices because of their relatively lower toxicity and simpler disposal requirements as compared to heavy metals (e.g. Pb, Hg, and Cd) [1]. Furthermore, SnS is considered as one of the most promising photoconverter materials in optoelectronic devices due to its high absorption coefficient ~10^5 cm^{-1} higher than the direct absorption edge 1.35 eV [2], earth abundant, cheap, and stable under ambient conditions [3]. In addition, the direct energy band gap would permit a high absorption coefficient and efficient electron–hole pairs generation under illumination [4], as well as its value would also allow a broad range of spectral absorption from ultraviolet to near infrared. It is essentially the combination of cation Sn, an element from group IV and anion S the element of group VI [5–7]. Moreover, SnS does not require extrinsic doping due to the intrinsic p-type conductivity by the formation of tin vacancies, which generate shallow acceptors levels within the band gap [8]. However, depending on Sn concentration, SnS manifests both the p and n-type conductivity or change its conductivity from p to n-type upon heat treatment [9], making it possible to prepare a SnS p-n homojunction [10]. The doping of SnS by Al, Cu, Cl increases its p-type conductivity by several orders of magnitude [11]. SnS is polymorphic and it can be mainly exhibited with three crystal structures of orthorhombic (α-SnS), zinc blende (ZB) and cubic [12,13]. The lattice constants of the orthorhombic structure comprises a = 0.4329 nm, b = 1.1193 nm and c = 0.398 nm [11,14], whereas, the lattice constants (a = b = c) of cubic and

zinc blende are 1.16 [15,16] and 0.5845 nm [3,17] respectively. In recent years, major efforts have been made in the characterization and synthesis of nanoscale semiconductor materials due to their unique properties (i.e., their ability to sense light and gas) [18]. The photodetectors are significant active elements for different scientific and industrial applications such as environmental monitoring, image sensing and communication [18,19]. Based on the wavelength range of operation, photodetectors are generally classified into two kinds of sub-systems: narrow band response detectors ultraviolet (UV), visible (Vis) and near infrared (NIR) and broadband response detectors [19].

1.2 Problem Statement

1. Grain boundary defect states trap majority carriers and give rise to potential barriers which impede the flow of current from one grain to the other [21]. Therefore, the grain boundaries cause that the photocurrent does not reach a steady state rapidly in both the rise and decay processes [22,23]. Hence, the low quality crystal structure of the thin film is not favourable for photodetector fabrication because of providing more grain boundaries. Therefore, this study uses a simple and inexpensive approach to enhance the crystallinity of the SnS thin film nanostructures by increasing the concentration of non-toxic trisodium citrate (complex agent).
2. A low dark current is essential in obtaining a high performance photodetector [24] because it enhances the signal to the noise ratio of the photodetector, given that shot noise is proportional to dark current [25]. Moreover, the low dark current as well indicates low detectability light intensity [26] and enhances the sensitivity of the photodetector [27–30]. In previous reports of SnS photodetectors based on

orthorhombic crystal structure on glass substrates, the dark current value was high in (μA) [31–33]. Increasing the pH value of solution reaction causes the transformation of the crystal structure of thin films from orthorhombic to cubic. This change in crystal structure causes a significant change in the magnitude of photodetector dark current from μA to nA of the.

1.3 Scope of Study

This study optimized the growth parameters of SnS nanostructures on glass substrates such as the concentration of complexing agent and pH. This study also optimized the growth parameter (pH) of SnS nanostructures on glass and PET substrates.

The optimized SnS nanostructures thin films synthesized on glass and PET substrates were used to fabricate high performance broadband photodetectors that can detect UV-Vis-NIR light illumination.

1.4 Objectives of thesis

The main objectives of this thesis can be summarized in the following points:

1. To optimize the crystallinity of SnS nanostructure by changing the concentration of complexing agent.
2. To determine the optimal pH value that controls the crystal structure (transition from orthorhombic to cubic) of the SnS thin films on glass and PET substrates for enhancing the photodetector performance.
3. To evaluate the performance of two UV-Vis-NIR photodetectors based on the SnS nanostructure on glass and PET substrates which depend on the optimum growth parameters.

1.5 Originality of Thesis

The originality of this research work involves the following aspects:

1. Control on phase, structural, morphology and optical properties by using various concentrations of non–toxic TSC as a complexing agent and pH values of a chemical reaction solution.
2. Growth and characterization of SnS thin film on flexible substrate PET by means CBD technique for the first time.
3. This work fabricates a high performance broadband spectral response of UV-Vis-NIR photodetectors on a glass and PET substrates, which have not been reported so far.

1.6 Thesis Outline

The thesis is organized into seven chapters. Chapter 1 includes a brief introduction of SnS nanostructures, and problem statement, the scope of the study, thesis objectives, and originality of thesis.

Chapter 2 presents a brief description of tin sulphide phases (SnS, SnS_2 and Sn_2S_3), and crystal structures of SnS phase. It also included a literature review of the growth of nanocrystalline SnS thin films by different technique and their the structural, optical and electrical properties. Theoretical background of thin films growth mechanism via CBD technique, and theoretical concepts on metal–semiconductor contacts and the working principles of the photodetector are also discussed in the chapter. Studies on nanostructured SnS-based photodetectors are also reviewed.

Chapter 3 describes the general principles of equipment and techniques utilized for the synthesis and characterizations of nanostructured SnS.

In Chapter 4, the effects of the various concentration of complex agent TSC on the structural, morphology, phase and optical characteristics of SnS nanostructures thin

films synthesized on glass substrates are investigated and presented. Based on the optimum concentration of TSC, the photoresponce characteristics of NIR photodetector are investigated.

Chapter 5, focuses on the, the influence of the various pH values on the structural, morphology, phase, optical and photoelectrical characteristics of SnS nanostructures thin films synthesized on glass substrates are also studied. Based on the optimum value of pH, the photoresponce characteristics of broadband response photodetector from UV to NIR are investigated.

Chapter 6 the influence of the various pH values on the structural, morphology, phase, optical and photoelectrical characteristics of SnS nanostructures thin films synthesized on PET substrates are investigated and presented. Based on the optimum value of pH, the photoresponce characteristics of broadband response photodetector from UV to NIR are investigated.

Finally, the conclusions of this study and recommendations for future works are presented in Chapter 7.

CHAPTER 2: LITERATURE REVIEW AND THEORETICAL BACKGROUND

2.1 Introduction

This chapter concisely explains the types and crystal structural properties of the different material phases of tin sulphide. This chapter also examines the influence of preparation parameters on the structural, phase, morphological variations and optical properties of synthesized tin sulphide film. In addition, this chapter evaluates studies related to the fabrication of SnS photodetector. Furthermore, the fundamental concepts and photoconduction mechanisms of in SnS photodetector and metal-semiconductor contact are discussed in this chapter.

2.2 Overview of Tin Sulphide

Tin sulphide is a challenging material to work with due to the ability of tin (Sn) to form two different oxidation states [34], Sn^{2+} ([Kr] $4d^{10}5s^{2}5p^{0}$) and Sn^{4+} ([Kr] $4d^{10}5s^{0}5p^{0}$) [35]. These two oxidation states allow tin sulphide to form different phases that are dependent on the material composition. As a result, there are multiple binary tin sulphides (SnS, SnS_2, Sn_2S_3, Sn_3S_4,…) [11,36–38]. The SnS, SnS_2, and Sn_2S_3 are main three discrete phases [37]. SnS and SnS_2 hold single oxidation states of Sn^{2+} and Sn^{4+}, respectively, while Sn_2S_3 contains a combination of Sn^{2+}, Sn^{4+}oxidation states with S_3 [35]. SnS_2 and Sn_2S_3 both exhibit n-type conductivity, [39–42] attributable to the dominant sulphur vacancy associated with the Sn^{4+} oxidation state [41]. On the contrary, SnS displays a native p-type conduction [43,44], derived from the formation of tin vacancies related to the Sn^{2+} oxidation state, which in turn generates shallow acceptors levels [8,45]. In addition, Sn_2S_3 display orthorhombic structure while SnS_2

exhibits hexagonal structure [46]. The crystal structure of SnS is discussed in the underlying section.

2.2.1 Literature Review of Tin Sulphide Phases

Tin sulphide phases have been studied in numerous studies by means of numerous techniques. For instance, Louise et al. [47] employed atmospheric pressure chemical vapour deposition technique to study the influence of substrate temperature within range of 300-545 °C on tin sulphide phase on glass substrates. The XRD patterns of the synthesized thin films within a temperature range of 300-500 °C revealed the presence of a single SnS_2 phase. Thin films synthesized at 525 and 545 °C exhibited Sn_2S_3 and SnS phases, respectively.

Calixto et al. [48] also studied the effect of substrate temperature in the range of 320– 488 °C on tin sulphide phase grown onto glass substrate via chemical spray pyrolysis. The XRD patterns of thin films synthesized between 320 and 455 °C displayed a distinctive peak corresponding to SnS phase with orthorhombic structure. In the patterns of thin films synthesized at 376 and 396 °C, two small peaks denoting the SnS_2 and Sn_2S_3 phases were also observed. For thin films were grown at 455 °C, the characteristic peak for SnS_2 phase was identified. With the increase in substrate temperature to 488 °C, the material is almost completely transformed to SnO_2.

In addition, Robles et al. [49] used the co-evaporation method to examine the effects of substrate temperature, within the range of (80-325 ^oC), on tin sulphide phases synthesized on soda-lime glass substrates. The XRD patterns of the thin films synthesized at lower temperatures (80–150 ^oC) showed characteristic peaks of SnS_2 phase with hexagonal structure, whereas distinctive peaks for SnS_2 and Sn_2S_3 phases were identified in the XRD patterns of the thin films at temperatures range of 150 and 250 ^oC. The XRD patterns of thin films grown at 325 ^oC show a distinct peak

corresponding to SnS phase with orthorhombic structure in addition to other peaks characteristic of the SnS_2 phase. Previous studies explored the different phases of tin sulphide thin films synthesized at high temperature.

In a similar study, Jayasree et al. [50] investigated the effect of complexing agent ethylene diamine tetra-acetic acid (EDTA) concentration on the phase of tin sulphide thin films synthesized using the CBD. The XRD patterns and Raman spectra results of the grown thin films synthesized with 0.05 M EDTA produced mixed phases of SnS and Sn_2S_3. The intensity of the Sn_2S_3 peak declines with an increase in EDTA concentration to 0.06 M, and then disappears as the EDTA concentration increases to 0.07 M and 0.08 M.

2.3 Overview of SnS Crystal Structure

The crystal structure of the inorganic nanocrystals plays an important role in controlling their chemical and physical properties [1]. The SnS belongs to the IV–VI group [51]. It is synthesized with Sn as the cation and S as the anion [6,7]. SnS is polymorphic and mainly exhibits three structures: α-SnS, cubic and zinc blende (ZB) [12,13]. The different crystal structures of SnS are shown in Figure (2-1). The lattice constants of α- SnS orthorhombic structure include a = 0.4329 nm, b = 1.1193 nm and c = 0.398 nm. It is constituted of double SnS layers perpendicular to the b axis, and Sn and S atoms are tightly bound within the layers and weak van der Waals bonds between the layers [5,11,14]. Whereas, the lattice constants (a=b=c) of zinc blende and cubic are 0.5845 [3,17] and 1.16 nm [15,16] respectively.

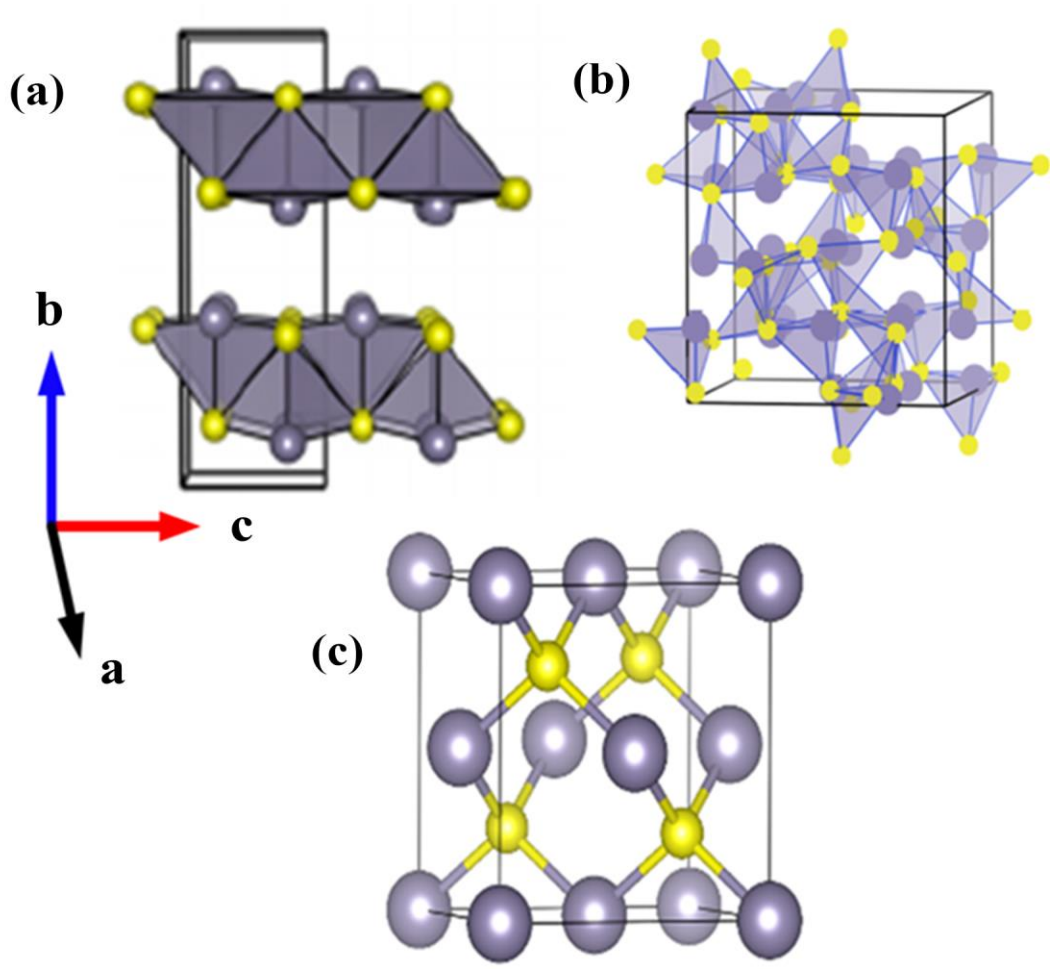

Figure 2.1: Different crystal structures of tin sulphide (a) orthorhombic [41], (b) cubic [52], (c) zinc blende [53].

2.4 Overview of pH Solution

The pH value of the deposition solution plays a significant role in defining the crystal structure, morphology, optical and electrical properties of the semiconductors films [9,29,31,54,55].

2.4.1 Literature Review of pH Solution

Ristov et al. also investigated the effect of pH (< 3, 3, 7, 10, 12 and > 12) on structural, morphology, optical and electrical properties using CBD technique. The results showed a weak adhesion of the film synthesized at pH < 3. At pH= 3, the film is bound tightly and cannot be easily detached. Film deposition is unattainable at pH

= 7 and > 12 because the growth rate is very small. The films deposition was achieved at temperature (80-90 ^{o}C). The XRD patterns of thin films showed orthorhombic crystal structure. Furthermore, the crystallinity and conductivity of the thin films increased at pH = 3, 10 and 12 [9].

Chao et al. [31] studied the effect of pH (5 and 6) on the crystal structure, morphology and electrical properties of SnS films under two different deposition times and temperatures using CBD. At pH 5, zinc blende crystal structure was achieved with temperature and deposition time of 35^{o}C and 10 h, respectively. The zinc blende structure evolved to an orthorhombic structure at pH 6. In addition, the thin films synthesized at 60 ^{o}C with deposition time 3 h showed orthorhombic structure at pH 5 and 6. The dark current of the zinc blende SnS film was lower compared to the orthorhombic SnS films. Furthermore, the SEM images of the SnS films showed that the zinc blende SnS film is characterized by a dense and continuous layer with nanosized islands while the orthorhombic SnS films were composed of short and spatially distributed cylindrical rods.

The effect of precursor solution pH on structural, morphology, optical and electrical properties in the range of 0.8 to 3.2 was examined by Sajeesh et al. via chemical spray pyrolysis (CSP) at a substrate temperature of 375 ± 5 ^{o}C [29]. The XRD patterns of thin films exhibited orthorhombic crystal structure. They discovered that the crystallinity and conductivity of SnS films increased with increasing pH value until attaining an optimum value, and subsequently decreased with increasing pH. Conversely, the energy band gap of the films exhibited a reverse behaviour. The SEM micrographs revealed an increase in the grains density with increasing pH. Moreover, the maximum photosensitivity (ratio of the photocurrent to the dark current) [56,57] was ~ 0.45.

Table 2.1 summarizes a comparison for the influence of pH value on crystal structure and photosensitivity of SnS thin films in previous studies [9,29,31]. The observations of the previous literatures show that all prepared thin films exhibited orthorhombic structure except the film prepared with pH 5 at temperature of 35 ^{o}C, which depicted zinc blende structure [31]. In other words, the pH value has no effect on the type of crystal structure when the deposition process is carried out at high temperature. This result may be attributed to the relationship between the type of crystal structure and growth rate of the films, whereby the high temperature deposition causes an increase growth rate [58,59], which consequently resulted in the orthorhombic structure. Moreover, the photodetector based on zinc blende structure showed higher photosensitivity compared to that of orthorhombic structure. This result may be attributed to low dark current of photodetector based on zinc blende structure; whereas, the photosensitivity tends to be higher for photodetector which is low in dark current [27–30].

Table 2.1: Comparison of the influence of pH value on crystal structure and photosensitivity of SnS thin films in previous studies.

Method	pH	Growth Temperature	Crystal Structure	Photosensitivity	Reference
CBD	3-12	80-90 ^{o}C	Orthorhombic	———	[9]
CBD	5	35 ^{o}C	Zinc blende	4.5	[31]
	6	35 ^{o}C	Orthorhombic	2.5	
	5	60 ^{o}C	Orthorhombic	———	
	6	60 ^{o}C	Orthorhombic	———	
CSP	0.8-3.2	375 ± 5 ^{o}C	Orthorhombic	Maximum ~ 0.45	[29]

2.5 Overview of Substrates

Generally, thin films have insignificant strength and cannot be made self-supporting. To ensure successful synthesis, the thin films must be deposited onto an appropriate supporting substrate material [60]. It is crucial to choose appropriate substrates that are structurally and chemically compatible with the film material, as regards temperature and stress stability [60]. Thus far, several substrate types have been used to synthesize SnS nanostructures by different techniques. The results showed that structural, surface morphology and optical properties of the fabricated SnS nanostructures are dependent on the substrate.

2.5.1 Literature Review of Substrates

Devika et al. [60] employed the thermal evaporation technique for the deposition of SnS thin films on glass, Ag-coated glass, ITO-coated glass and Si wafer substrates. The XRD results revealed that the dominant peak depends on the type of substrate. Furthermore, the crystallite sizes of the dominant peak were 168.3, 171.6, 180, and 220.1 A^o for glass, Ag-coated glass, Si wafer, and ITO-coated glass substrates respectively. In addition, the surface morphological features of glass and Ag-coated glass substrates are similar but different for the ITO-coated glass and Si wafer substrates. Moreover, The SnS films deposited on glass, Si wafer, ITO-coated glass, and Ag-coated glass show an energy band gap of 1.35, 1.55, 1.62, and 1.86 eV, respectively.

Thierno et al. [61] synthesized SnS thin films on bare glass, ITO-coated glass, and Mo-coated glass substrates via chemical spray pyrolysis (CSP) at 350 ^oC. The XRD analysis revealed that the thin film deposited onto glass substrate has a relatively larger crystallites size value than the other substrates. They attributed this variation in crystallites size to the better crystallinity of thin films deposited onto glass substrate

compared to Mo coated and ITO-coated glasses. In addition, Raman analysis revealed similar vibrational modes of SnS for all the deposited thin films with only slight differences in the Raman signal intensity. Furthermore, energy band gap values of 1.64, 1.74 and 1.82 eV were obtained for SnS films deposited on glass, Mo-coated glass and ITO-coated glass, respectively.

Table 2.2 summarizes a comparison for the influence of substrates on crystallite size and energy gap of SnS thin films in previous studies [60,61]. The observations of the previous literatures show that the dependence of crystallite size and energy band gap of thin films on the substrate. For thermal evaporation, the glass substrate has lower value of crystallite size while for the CSP on glass substrate has higher value. These results might be attributed to different methods used in the deposition process.

Table 2.2: Comparison of the influence of substrate on crystallite size and energy gap of SnS thin films in previous studies.

Method	Substrate	crystallite size (A^o)	Energy band gap (eV)	Reference
Thermal Evaporation	glass	168.3	1.35	[60]
	Ag-coated glass	171.6	1.55	
	ITO-coated glass	220.1	1.62	
	Si wafer	180	1.86	
CSP	glass	459	1.64	[61]
	ITO-coated glass	180	1.74	
	Mo-coated glass	160	1.82	

2.6 Overview of Chemical Bath Deposition Technique

Recently, nanoscale semiconductor materials have attracted considerable attention due to their excellent properties (i.e., their ability to detect light and gas). These materials have an extensive array of applications such as the manufacture of photodetectors [18,62], phototransistors [63,64] and gas sensors [65]. Numerous techniques have been utilized to synthesize SnS nanostructures on different kinds of substrates, and they include electrodeposition [66,67], thermal evaporation [68–71] successive ion layer adsorption and reaction method (SILAR) [11,72], RF magnetron sputtering [73], electron beam deposition [74,75], spray pyrolysis [10,29,48], chemical vapor deposition [47] and CBD [6,31,50,76–86]. From these different techniques, CBD has been widely exploited for the synthesis of SnS nanostructures because it is the experimentally least complex technique in chemistry and material science since it does not require highly technical instrumentation and costly equipment. In addition, it does not need high temperature to synthesize the reaction between the dissolved precursors. Generally, the temperature of aqueous solution used in CBD to synthesize SnS ranges from room temperature to 90 ºC [87]. Various substrates such as metals, semiconductors and insulators can be used because of their low susceptibility to oxidation and corrosion at low temperature [88,89]. Furthermore, the relatively low temperature deposition using CBD is suitable for the growth of SnS nanostructures on flexible substrates such as PET. Based on these several advantages, the CBD technique was selected for the synthesis of semiconductor thin films.

2.6.1 Mechanism of Chemical Bath Deposition Technique

The formation of a film on a substrate from a solution involves two steps:

nucleation and particle growth [43,89]. Moreover, (CBD) involves the controlled precipitation of a solid phase from their precursor ions in the reaction bath containing

the aqueous solution. The control of precipitants is a crucial factor in the deposition of the good quality thin film as well as the adherence to appropriate substrates. For this reason, a complexing agent is normally used, which binds with the free metal ions ($Sn^{2+)}$ in the solution to produce Sn-complexing ions. Under suitable conditions, the Sn-complexing ions undergo decomposition to release the Sn^{2+} ions that formerly bond with S^{2-} ions existent in the solution to form a solid phase (SnS). The complexing agent ensures to avoid rapid precipitation of the solid phase and enhances the synthesis of a homogenous SnS thin film on the substrate [59]. There are two effective mechanisms in nucleation and film growth, and they include ion by ion (simple and complex-decomposition) and cluster by cluster (simple and complex-decomposition) [43,59,87,90]. These mechanisms are explained separately in the underlying sub-sections.

2.6.1(a) Simple Ion-by-Ion mechanism

In this mechanism, Sn and S ions are diffused to the substrate to form the SnS nucleus. The nucleation process is catalyzed by the substrate. SnS nuclei are grown via the adsorption of Sn and S ions from the solution and the nucleation of new crystals. The growth of SnS crystals continues until the precursors in the solution are entirely depleted. The simple ion by ion mechanism is expressed by the equation below [31].

$$Sn^{2+}+S^{2-}\rightarrow SnS \qquad (2\text{-}1)$$

A complex agent is added to control the number of ions and reaction rate, in addition to prevent the hydroxide from precipitating out [59].

2.6.1(b) Complex-Decomposition Ion-by-Ion Mechanism

In this mechanism, the complexation of a free Sn^{2+} ion by thioacetamide to give a Sn-thioacetamide complexion [59].

$$Sn^{2+} + H_3C.C(S)NH_2 \rightarrow [H_3C.C(S)NH_2\text{-}Sn]^{2+} \qquad (2\text{-}2)$$

By breaking the S-C bond, this ion is hydrolyzed to form SnS [59].

$$[H_3C.C(S)NH_2\text{-}Sn]^{2+} + 2OH^- \rightarrow SnS + CH_3CONH_2 + H_2O \quad (2\text{-}3)$$

2.6.1(c) Simple Cluster (Hydroxide) Mechanism

The deposition of SnS thin films via hydroxide aggregation mechanism involves the diffusion and adherence of hydroxide colloidal particles to the substrate. The adhering hydroxide colloids subsequently react with S ions, which results in an exchange between sulphide and hydroxide ions. The exchange reaction can occur both on the substrate and in the solution and continues until most of the hydroxide are converted to sulphide. Afterward, the first SnS particles bond with each other to form an aggregated film. The hydroxide cluster mechanism is expressed by the equation below [31,90]:

$$Sn^{2+} + 2OH^- \rightarrow Sn(OH)_2 \quad (2\text{-}4)$$

$$Sn(OH)_2 + S^{2-} \rightarrow SnS + 2OH^- \quad (2\text{-}5)$$

2.6.1(d) Complex-Decomposition Cluster Mechanism

This mechanism is based on the formation of solid phase instead of reacting directly with a free anion (S); it forms an intermediate complex with the anion-forming reagent [90]. Continuing with SnS deposited from a thioacetamide bath by considering example given as [59].

$$Sn^{2+} + 2OH^- \rightarrow Sn(OH)_2 \quad (2\text{-}6)$$

$$Sn(OH)_2 + H_3C.C(S)NH_2 \rightarrow Sn(OH)_2.H_3C.C(S)NH_2 \quad (2\text{-}7)$$

This complex then decomposes via the break of the thioacetamide S-C bond, leaving the S bond to Sn [59].

$$Sn(OH)_2.H_3C.C(S)NH_2 \rightarrow SnS + CH_3CONH_2 + H_2O \quad (2\text{-}8)$$

2.6.2 Literature Review of Chemical Bath Deposition

The influence of growth time (2, 4, 6 and 8 h) on structural, optical and electrical properties of SnS thin films has been investigated in an earlier study [43]. The XRD patterns obtained in the study showed that the films were polycrystalline and orthorhombic in structure except for those subjected to only 2 h of growth, which are amorphous. The grain size, texture coefficient and conductivity were found to increase with increasing growth duration until 6 h, and afterward began to decrease with increasing growth time. Direct energy band gap values of 1.3-1.97 eV were measured for the SnS thin films.

Tanusevski [76] also studied the effect of annealing temperature on the structural, electrical and optical characteristics of prepared thin film. The deposition procedure was performed at room temperature for the duration of 18 h at pH 7. The thickness of the deposited thin films was 340 nm after a single stage of deposition. The film thickness of approximately 680 nm was obtained by repeating the deposition process a second time. XRD patterns indicated that the 680 nm thick films as-prepared and thermally treated at 300 ^{o}C for 1 h in argon atmosphere are polycrystalline with orthorhombic crystal structure. Furthermore, heat treatment of the thin films at 300 ^{o}C increased the peak height of the preferential orientation while the thermal treatment in argon at 250 ^{o}C for 1 h and 8 h unaffected the crystallinity of thin films. The study also revealed that photoconductivity increased under thermal treatment. Furthermore, the direct energy band gap is not changed thermal treatment.

David et al. [91] employed CBD for the deposition of SnS thin film on microscope glass substrates at 25 ^{o}C for a duration of 6 h. They stated that thickness of the synthesized film increased from 100 nm to approximately 450 nm by four successive deposition procedures. In addition, XRD patterns of the films showed that

zinc blende is the main crystalline

Y. Jayasree et al. [92] studied the effect of concentration of complexing agent triethanolamine (TEA) on the structural, morphological and optical properties of SnS thin films. XRD patterns were obtained for films prepared at room temperature for 90 min with different TEA concentrations. The patterns of films obtained from a bath with 1.75 M TEA displayed peaks corresponding to SnS and Sn_2S_3 phases, while the patterns of films prepared with 1.85 M TEA exhibit polycrystalline and single phase SnS. Increasing the concentration of TEA to 1.95 M produced amorphous films. All XRD patterns of the films indicated orthorhombic crystal structure. In addition, the surface morphology of films prepared with various concentrations of TEA revealed that microstructure of films with TEA 1.75 M was discontinuous nature of films whereas films deposited at TEA 1.85 M were well defined grain morphology with cluster formations and with further increasing the concentration of TEA to 1.95 M, grain cluster size decreases. Furthermore, the direct energy band gap values were 1.75, 1.5 and 1.4 eV at concentration of TEA 1.75, 1.85 and 1.95 M respectively.

In a similar study, Jayasree et al. [50] investigated the effect of complexing agent ethylene diamine tetra-acetic acid (EDTA) concentration on the structural, phase, and optical properties of tin sulphide thin films synthesized using the CBD. All peaks in the XRD patterns thin films were indexed to the orthorhombic crystal structure. In addition, the XRD patterns and Raman spectra results of the grown thin films synthesized with 0.05 M EDTA produced mixed phases of SnS and Sn_2S_3. The intensity of the Sn_2S_3 peak declines with an increase in EDTA concentration to 0.06 M, and then disappears as the EDTA concentration increases to 0.07 M and 0.08 M. The direct energy band gap values were found 1.67, 1.63, 1.55 and 1.65 eV for complexing agent concentrations of 0.05, 0.06, 0.07 and 0.08 M, respectively.

Gode et al. [82] studied the effect of concentration of complexing agent TSC (0.0064, 0.0072, and 0.0080 M) on structural, electrical and optical properties of SnS films. They discovered that the average size and thickness of thin films increased with increasing concentration of TSC. The conductivity, carrier concentration and mobility of the films also increased, although slightly, with increasing concentration of trisodium. Conversely, the direct energy band gap decreased from 1.40 eV to 1.17 eV with increasing concentration of TSC.

He. et al. [93] investigated the influence of time and temperature on thickness and energy band gap of thin films. 0.1 M stannous chloride ($SnCl_2.2H_2O$) and 0.15 M of thioacetamide (C_2H_5NS) were used as sources of Sn^{2+} and S^{2-} ions, respectively. 0.15 M of disodium citrate ($Na_2C_6H_6O_7$) was used as the complexing agent. The pH of the bath was adjusted to pH~ 6. The XRD of prepared thin films revealed orthorhombic structure, and the crystallinity of thin films increased with increasing temperature and time. The thickness of films deposited for 1 h were found to be 70, 170, and 400 nm at temperature of 60, 70, and 80 ^oC, respectively, whereas, the thickness of films deposited for 2 h were found to be 120, 300, and 650 nm at temperature of 60, 70, and 80 ^oC, respectively. Furthermore, the energy band gap varies between 1.46-1.62 eV for deposition of 1 h; whereas, the energy band gap varies between 1.45-1.52 eV at deposition time of 2 h.

Similarly, Ana et al. [94] studied the effect of temperature on the crystalline structure, thickness and electrical properties of SnS thin films prepared on the glass substrate via CBD. The deposition procedure was performed at bath temperatures of 20, 30, 35 and 40 ^oC. The initial pH of the solution was around 11 and the time of deposition was 24 h. They discovered that the films prepared at 20 and 30 ^oC were primarily cubic crystalline structure with the insignificant presence of orthorhombic

crystals, whereas, thin films prepared at 35 ^{o}C and above are characterized by orthorhombic crystalline structure. In addition, thicknesses of 230 and 600 nm were obtained for thin films prepared at 20 and at 40 ^{o}C respectively for the same duration. Furthermore, electrical conductivity values of 10^{-7} $(\Omega.cm)^{-1}$ and 10^{-4} $(\Omega\ cm)^{-1}$ were obtained for cubic structured films and orthorhombic structured films, respectively. structure whereas orthorhombic structure is the minor crystalline arrangement.

Chalapathi et al. [13] studied the effect of complex agent EDTA concentration (0.075 M to 0.125 M) on the properties of thin films synthesized on a glass substrate. The deposition was executed for a duration of 6 h, pH 10.5 and 45 ^{o}C. The XRD analysis of the thin films revealed cubic crystal structure with lattice parameter a = 1.158 nm. The crystallite size and direct energy band gap increased from 46 nm to 60 nm and from 1.67 eV to 1.73 eV, respectively, with increasing EDTA concentration. Raman spectroscopy analysis of the thin films indicated the existence of a secondary SnS_2 secondary phase. The thickness of the thin films also increased from 500 nm to 620 nm with increase in EDTA concentration.

Nair et al [95] synthesized thin films with orthorhombic and cubic crystal structures. The study reported that the measured energy band gaps were indirect (1.1 eV) and direct (1.66 eV) for orthorhombic and cubic structure, respectively. In addition, the conductivity of orthorhombic thin film is two orders higher than cubic.

Table 2.3 summarizes a comparison for the influence of complex agent concentration on crystallinity size, phases and energy gap of tin sulphide thin films in previous studies [50,82,92]. The observations of the previous literatures reveal the dependence of crystallinity, phase, and energy band gap of thin films on the concentration. In general, the crystallinity increased with an increase in the concentration of complex agent, whereas, the energy band gap decreased.

Furthermore, the peak of Sn_2S_3 phase declined with an increase in the concentration of complex agent.

Table 2.3: Comparison of the influence of complex agent concentration on crystallinity, phases and energy gap of tin sulphide thin films in previous studies.

Complex Agent	Concentration	Crystallinity	Phase	Energy band gap (eV)	Reference
TEA	1.75 M	Increased with increasing concentration of TEA	SnS and Sn_2S_3	1.75	[92]
	1.85 M		SnS	1.50	
	1.95 M		amorphous	1.4	
EDTA	0.05 M	Increased with increasing concentration of EDTA and optimum at concentration 0.07 M	SnS and Sn_2S_3	1.67	[50]
	0.06 M		SnS and Sn_2S_3	1.63	
	0.07 M		SnS	1.55	
	0.08 M		SnS	1.65	
TSC	0.0064 M	Increased with increasing concentration of TSC	———	1.4	[82]
	0.0072 M		———	1.28	
	0.0080 M		———	1.1	

2.7 Overview of Photodetection Based on SnS Nanostructures

The main physical mechanism of photoconductivity is based on photon absorption of light incident on a semiconductor. The photon energy is sufficient to excite an electron from valence band to conduction band, which changes the electric attributes of the electronic system [96], such as the generation of photocurrent in a photodetector or a photovoltage in a photovoltaic detector. For light detection, different kinds of photodetectors have been fabricated such as photoconductor [97], metal–semiconductor–metal (MSM) structure [98], the p–n junction [99] and Schottky diode [100]. Among them structures, the MSM photodetector has garnered the most

attention, because of its basic structural design, cost effective wafers, intrinsic high speed and simplicity of optoelectronic integration [100,101]. MSM is a prominently used photodetector in military and civil applications [100].

2.7.1 Literature Review of SnS Photodetector

Chao et al. [31] investigated the impact of crystal structures on the photoresponse characteristics of SnS thin film deposited on glass substrate. They fabricated two photodetector devices based on orthorhombic and zinc blende crystal structures. Two devices were subjected to tungsten - halogen illumination of 100 mW/cm^2. The results revealed that the light current to dark current ratios were about 3.5 at bias voltage of 10 V and 5.5 at a bias voltage of 20 V for orthorhombic and zinc blende SnS films, respectively.

Fangyuan et al. used the hydrothermal technique to synthesize SnS thin films [18]. The procedure was conducted at 180 ^oC and for a duration of 24 h. The photodetector was fabricated via re-dispersion of the synthesized SnS in ethanol ultrasonication, which was then spun on the surface of Si substrate covered with a dielectric layer of SiO_2. A pair of gold (Au) electrodes was evaporated on the SnS using a gold-wire mask moving technique. The gap between the electrodes was measured at 30 µm. The photodetector device was subjected to light illumination of 650 nm at bias voltage 0.1 V. The device exhibited increasing the current under illumination and with sensitivity of approximately 28%. In addition, rise and decay time of 0.45 and 0.56 s were determined for the photodetector device, respectively.

In a different study, Jun et al. [33] synthesized large size SnS thin crystals using solvothermal technique. The study fabricated the SnS photodetector by depositing thin crystals on the surface of a highly doped n-type Si substrate covered with a dielectric layer of 300 nm silicon dioxide (SiO_2) substrate. Layers of Cr (30 nm)/Au (120 nm)

alloy were subsequently deposited on the SiO_2 layer by thermal evaporation. Four lasers with various wavelengths (405, 445, 532 and 632 nm) and light illumination of 50 mW/cm^2 were used as the illumination sources for the device. The wavelength 532 nm showed the highest photodetection compared to other wavelengths. In addition, the sensitivity of approximately 130% was achieved, for illumination under 532 nm and bias voltage of 2 V.

Srinivasa et al. [102] examined the effect of thickness on the electrical properties of thin films deposited on glass substrates. The co-evaporation technique was used to deposit thin films within the thickness range of 170 nm to 915 nm. The XRD patterns showed orthorhombic crystal structure. The results revealed that the electrical conductivity and photoconductivity of the films increase by more than two orders with an increase of film thickness from 170 nm to 915 nm. The sensitivity values were 84%, 55%, 25% and 32% for the film thickness 170, 280, 426 and 915 nm respectively, at the bias voltage of 5V and visible light intensity of 100 mW/cm^2.

Junfeng et al. [12] performed the first attempt to deposit SnS nanostructure on PET. The deposition process involved the synthesis of SnS nanoribbons via a facile polyol refluxing process. The as-prepared SnS nanoribbon was then dispersed in ethanol containing a small quantity of terpineol and ethylene cellulose. The materials were subsequently stirred to form a homogenous distribution paste. Afterward, the paste was deposited onto the PET substrate. Silver parallel electrodes were deposited on the substrates for the fabrication of a flexible detector. Using Xenon lamp as a source of illumination, the photodetector showed that the ratio of current under illumination to dark was 22 at bias voltage of 10 V and illumination intensity of 300 mW/cm^2. Rise and decay time of 5.4 and 1.8 s were measured, respectively.

Table 2. 4 summarizes a comparison for the fabricated photodetectors based on SnS thin films in previous studies [12,18,31,33,102]. The observations of the previous literature revealed that the fabricated photodetector based on zinc blende structure exhibited the photosensitivity highest compared to that of orthorhombic structure for rigid substrates (glass and SiO_2/Si). Moreover, the fabricated photodetector on the PET substrate showed the photosensitivity highest compared to that of glass and SiO_2/Si substrates.

Table 2.4: Comparison of the SnS photodetectors photosensitivity in previous studies.

Method	Substrate	Crystal Structure	Illumination Source	Light Intensity (mW/cm^2)	Photosensitivity	Reference
CBD	glass	Zinc blende	Tungsten halogen lamp	100	4.5	[31]
	glass	Orthorhombic	Tungsten halogen lamp	100	2.5	[31]
Co-evaporation	glass	Orthorhombic	Visible light	100	0.84	[102]
Hydrothermal	SiO_2/Si	Orthorhombic	650 nm	———	0.28	[18]
Solvothermal	SiO_2/Si	Orthorhombic	532 nm	50	1.3	[33]
Refluxing process	PET	Orthorhombic	Xenon lamp	300	21	[12]

2.7.2 Theoretical Concept of Photodetector

Photodetector is a semiconductor device that can convert incident light energy into a detectable electrical signal, when the photon energy is higher or equal compared to the semiconductor energy gap. Photons absorption by the semiconductor material results in the generation of free electrons in the conduction band excited from the valence band. Simultaneously, holes are generated in the valence band. The photo-excitation of electron–hole pairs is illustrated in Figure 2.2 [103].